

Journal of Mechanics of Materials and Structures

**A PULL-OUT MODEL FOR PERFECTLY BONDED CARBON NANOTUBE
IN POLYMER COMPOSITES**

Khondaker Sakil Ahmed and Ang Kok Keng

Volume 7, No. 8-9

October 2012



A PULL-OUT MODEL FOR PERFECTLY BONDED CARBON NANOTUBE IN POLYMER COMPOSITES

KHONDAKER SAKIL AHMED AND ANG KOK KENG

A pull-out model for carbon nanotube (CNT) reinforced composite is presented to obtain the interface characteristic in which perfect bonding at the interface is considered. In the model, a partially embedded CNT in a cylindrical polymer matrix is subjected to an axial load at the open end. By using representative volume element (RVE) concept, analytical solutions are derived for axial and interfacial shear stresses in the CNT. Parametric studies are also conducted to obtain the influence of aspect ratio, modulus ratio and relative size of RVE on stress components. Variation of critical pull-out stress with embedded length and CNT/polymer Young's modulus ratio are also investigated.

1. Introduction

One of the major applications of carbon nanotube is its use as high strength reinforcements for high performance composite materials [Ajayan et al. 2000; Frankland and Harik 2003; Haque and Ramasetty 2005; Qian et al. 2000; 2002; Thostenson et al. 2001; Tserpes et al. 2008; Wang et al. 2008]. Many factors affecting the performance of CNT-reinforced composites include [Ailin et al. 2010] mechanical properties of nanotubes as well as matrix, purity, interface characteristics such as interfacial bonding, interactions with host and orientation of CNTs in the matrix. Similar to conventional composites, many research studies also suggested that the performance of CNT-reinforced composites depends critically on the interfacial characteristics between CNT and the matrix material [Kin and Sean 2001; Liao and Li 2001; Manoharan et al. 2009; Qian 2003; 2000; Salehikhojin and Jalili 2008; Wang et al. 2008].

One of the major challenges in the CNT-reinforced composites is load transfer efficiency across the CNT/matrix interface. Research studies suggest that the main contributing factors for interfacial load transfer between CNT and polymer are mechanical interlocking (friction), chemical bonding and noncovalent bonding like $v dW$ interactions [Haque and Ramasetty 2005; Jiang et al. 2006; 2008].

In the literature, several researchers also found the presence of strong bonding at the interface when nanotubes were dispersed in PHAE or polystyrene [Qian et al. 2000; 2002]. Chemical bonding or surface treatment is difficult between CNT and polymer matrix but it certainly improves the interface strength by a significant order. As an example, chemisorptions to as little as 5.0% of the nanotube carbon atoms increases the shear stress of at the interface by about 1000% [Zheng et al. 2008]. It is also well known that surface to volume ratio (SVR) and aspect ratio (AR) of nanotubes are higher in magnitudes than those of traditional composites. Though there is a huge difference in strength between nanotube and polymer matrix, high frictional forces may prevent slipping of the tube and ensure good load transfer even in chemically nonbonded CNT/matrix interface. Therefore, all the aforementioned properties of CNT ensure that weak CNT/matrix interface can also be assumed as perfectly bonded.

Keywords: perfectly bonded interface, representative volume element, stress transfer, aspect ratio, critical pull-out stress.

In conventional fiber-reinforced composites [Cox 1952; Kim and Mai 1998; Li-Min et al. 1992], pull-out tests are widely used to measure the interface characteristics, stress distributions, maximum pull-out force or effective pull-out length. However, it is very difficult to conduct experimental pull-out tests on CNT embedded in polymer matrix due to the challenges involved in gripping, manipulation and stress, strain measurements. The load transfer mechanism in conventional fiber-reinforced composites has been studied by using the pull-out model for many years [Li-Min et al. 1992; Seshadri and Saigal 2007]. Some researchers have conducted molecular dynamic (MD) simulations [Frankland and Harik 2003; Kin and Sean 2001] on CNT pull-out models. Though MD simulation is generally accepted to be more accurate, it is however highly time consuming and costly.

Recently, some researchers have proposed various pull-out models for CNT-reinforced composites using continuum mechanics approach [Ahmed and Ang 2010; Kin-tak 2003; Natsuki et al. 2007; Tan and Kin 2004]. A number of previous studies have considered the case of frictionally bonded interface that are valid only for very weak CNT/matrix interface. In [Wagner 2002], the interfacial shear strength in polymer composites reinforced by SWNT has been estimated using a modified Kelly–Tyson approach which however assumes the interfacial shear and axial normal stresses to be uniform. A perfectly bonded CNT/matrix interface using RVE concept was considered in [Gao and Li 2005]. This study, however, was on a shear lag model which assumes the CNT to be fully embedded within the matrix and is aimed at estimating the average stress components of the matrix and CNT. On the other hand, a pull-out test model is designed to estimate the critical pull-out force, the mechanism of stress transfer from CNT to matrix as well as the factors that influence the composite behavior. Surprisingly, no research study on CNT pull-out model has been reported in the literature for perfectly bonded interface.

The main objective of the current work is to develop an analytical pull-out model of a perfectly bonded CNT/matrix using linear elasticity theory. The proposed continuum-based model is capable of predicting axial and interfacial shear stress distributions of the CNT as well as the critical pull-out force. Analytical results obtained from the model are verified by comparing with those available in the literature. To illustrate the application of the proposed model, parametric studies are conducted to examine the effects of aspect ratio, radius ratio and modulus ratio on the average axial and interfacial shear stresses in CNT. Therefore, this model aims to provide a more convenient solution that would help to provide a design guideline for stress transferring of CNT in composites.

2. Proposed pull-out model

In this study, a 3D cylindrical representative volume element (RVE) is selected from a cracked section of CNT-reinforced composite shown in Figure 1(a) to define the pull-out model, as shown in Figure 1(b). The pull-out model comprises of a CNT of radius a partially embedded within a cylindrical matrix of radius b . The z and r coordinates are assigned along the axial and radial directions of the CNT, respectively. The embedded length of the CNT in the polymer matrix is denoted by L and F is the axial normal force applied at the open end of the CNT.

To investigate the pull-out characteristics of the CNT, it is proposed that the CNT be replaced by an effective solid fiber having the same length and outer diameter as shown in Figure 1(c). The modulus of the effective fiber E_f can be expressed in terms of the elastic modulus of the nanotube E_t as follows

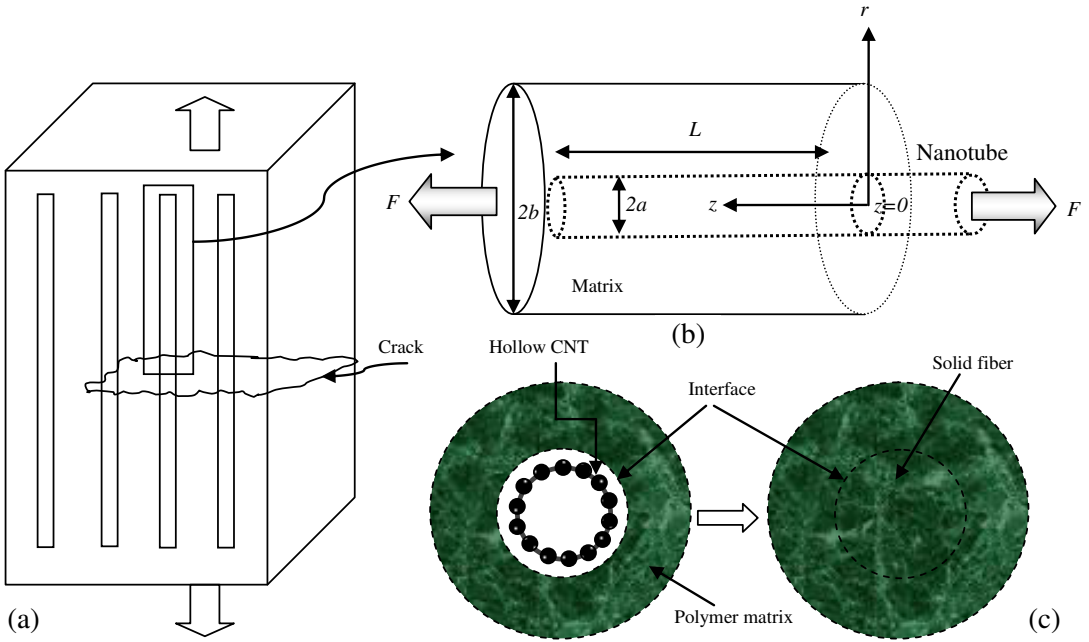


Figure 1. Schematics of the CNT pull-out model: (a) cracked section of CNT-reinforced composite; (b) partially embedded CNT in 3-D RVE; (c) conversion of typical hollow CNT to equivalent effective fiber in polymer matrix.

(see [Ailin et al. 2010; Gao and Li 2005; Thostenson et al. 2001]):

$$E_f = \frac{A_t}{A_{eff}} E_t = \frac{2at - t^2}{a^2} E_t; \tag{1}$$

this is determined by setting the cross-sectional areas of the hollow CNT and solid fiber to be equal to each other. Here, t denotes the thickness of the nanotube.

The governing equilibrium equations for the axisymmetric problem in terms of polar coordinates (r, θ, z) may be written as

$$\frac{d\sigma_{rr}}{dr} + \frac{d\tau_{rz}}{dz} + \frac{\sigma_{rr} - \sigma_{\theta\theta}}{r} = 0, \quad \frac{d\sigma_{zz}}{dz} + \frac{1}{r} \frac{d(r\tau_{rz})}{dr} = 0, \tag{2}$$

where $\sigma_{zz}, \sigma_{rr}, \sigma_{\theta\theta}, \tau_{rz}$ are the axial, radial, hoop and shear stress components, respectively, $\epsilon_{rr}, \epsilon_{zz}, \epsilon_{\theta\theta}, \gamma_{rz}$ the corresponding strain components, respectively and w, u the axial and radial displacements, respectively.

Assuming that the material obeys Hooke’s law, the constitutive equations may be written as

$$\epsilon_{zz} = \frac{1}{E} \{\sigma_{zz} - \nu(\sigma_{rr} + \sigma_{\theta\theta})\}, \quad \epsilon_{rr} = \frac{1}{E} \{\sigma_{rr} - \nu(\sigma_{zz} + \sigma_{\theta\theta})\}, \quad \epsilon_{\theta\theta} = \frac{1}{E} \{\sigma_{\theta\theta} - \nu(\sigma_{rr} + \sigma_{zz})\}, \tag{3a}$$

$$\gamma_{rz} = \frac{\tau_{rz}}{G}, \tag{3b}$$

where E, G and ν are the Young’s modulus, shear modulus and Poisson’s ratio, respectively.

The strain-displacement relationships may be written as

$$\epsilon_{rr} = \frac{du}{dr}, \quad \epsilon_{zz} = \frac{dw}{dz}, \quad \epsilon_{\theta\theta} = \frac{u}{r}, \quad \gamma_{rz} = \frac{du}{dz} + \frac{dw}{dr}. \tag{4}$$

Note that Equations (2)–(4) are valid for both the effective solid fiber and matrix.

The mechanical equilibrium equation at any section of the RVE can be written as

$$\pi a^2 \sigma = \int_0^a \sigma_{zz}^f(2\pi r) dr + \int_a^b \sigma_{zz}^m(2\pi r) dr, \tag{5}$$

where $\sigma (= F/\pi a^2)$ denotes the average stress applied in the effective fiber at $z = 0$. (Superscript f and m refer to the effective fiber and matrix, respectively.) The average axial stresses of CNT and matrix can be expressed as

$$\bar{\sigma}_{zz}^f = \frac{2}{a^2} \int_0^a \sigma_{zz}^f r dr, \quad \bar{\sigma}_{zz}^m = \frac{2}{b^2 - a^2} \int_a^b \sigma_{zz}^m r dr. \tag{6}$$

The boundary conditions of the pull-out model are

$$\begin{aligned} \bar{\sigma}_{zz}^f(0) = \sigma, \quad \bar{\sigma}_{zz}^f(L) = \bar{\sigma}_{zz}^m(L), \quad \tau_{rz}^f(a) = \tau_i, \quad \tau_{rz}^m(b) = 0, \\ \bar{\sigma}_{rr}^m(b) = 0, \quad \epsilon_z^f(a) = \epsilon_z^m(a), \quad w_z^f(a) = w_z^m(a), \end{aligned} \tag{7}$$

where τ_i is the interfacial shear stress.

Upon integrating (2)₂ with respect to r from 0 to a and applying the boundary conditions given in (7)₃ for the effective fiber, we obtain

$$\frac{d\bar{\sigma}_{zz}^f}{dz} = -\frac{2}{a} \tau_i. \tag{8}$$

In view that the matrix shear stress (τ_{rz}^m) has to be compatible with interfacial shear stress (τ_i) and the fact that the outer surface of matrix cylinder is stress free, τ_{rz}^m at any radial distance r can be derived by integrating (2)₂ to give

$$\tau_{rz}^m = \frac{a}{b^2 - a^2} \frac{(b^2 - r^2)}{r} \tau_i. \tag{9}$$

Since $\frac{du}{dz} \ll \frac{dw}{dr}$, we can assume $\frac{du}{dz} + \frac{dw}{dr} \equiv \frac{dw}{dr}$. Therefore, (4)₄ may be rewritten as

$$\gamma_{rz} = \frac{dw}{dr}. \tag{10}$$

In view of (10), Equation (3b) for both the fiber and matrix may then be rewritten as

$$\tau_{rz}^f = \frac{E_f}{1 + \nu_f} \frac{dw^f}{dr}, \quad \tau_{rz}^m = \frac{E_m}{1 + \nu_m} \frac{dw^m}{dr}. \tag{11}$$

By substituting (11)₂ into (9), we obtain

$$\frac{E_m}{1 + \nu_m} \frac{dw^m}{dr} = \frac{\gamma}{a} \frac{(b^2 - r^2)}{r} \tau_i, \tag{12}$$

where

$$\gamma = \frac{a^2}{b^2 - a^2}. \tag{13}$$

By integrating (12) from a to b , we obtain

$$\tau_i = \frac{a}{\gamma} \frac{E_m(w_b^m - w_a^m)}{(1 + \nu_m)(b^2 \ln \frac{b}{a} - a^2/2\gamma)}. \tag{14}$$

Finally, by substituting (14) into (12) and integrating from a to b , we obtain

$$w^m(r, z) = w_a^m + \frac{(b^2 \ln \frac{r}{a} - (r^2 - a^2)/2)(w_b^m - w_a^m)}{b^2 \ln \frac{b}{a} - a^2/2\gamma}. \tag{15}$$

Since the axial stress is the predominant stress component, we assume that $\sigma_{rr} + \sigma_{\theta\theta} \ll \sigma_{zz}$. Equation (3a)₁ may therefore be rewritten as

$$\sigma_{zz}^f = E_f \frac{dw^f}{dz}, \quad \sigma_{zz}^m = E_m \frac{dw^m}{dz}. \tag{16}$$

Equation (16)₂ becomes, in view of (15),

$$\sigma_{zz}^m(r, z) = \sigma_{zz}^m(a, z) + \frac{\{b^2 \ln \frac{r}{a} - (r^2 - a^2)/2\} \{\sigma_{zz}^m(b, z) - \sigma_{zz}^m(a, z)\}}{b^2 \ln \frac{b}{a} - a^2/2\gamma}. \tag{17}$$

Upon substituting (17) into (5) and after rearranging, we obtain

$$\sigma_{zz}^m(b, z) = \frac{\sigma - \gamma(\bar{\sigma}_{zz}^f - \sigma)}{\beta} + \left(1 - \frac{1}{\beta}\right) \sigma_{zz}^m(a, z) \tag{18}$$

where

$$\beta = \frac{b^2(1 + \gamma) \ln \frac{b}{a} - (3b^2 - a^2)/4}{b^2 \ln \frac{b}{a} - a^2/2\gamma}. \tag{19}$$

Now, by substituting (14) into (8), we obtain

$$\frac{d\bar{\sigma}_{zz}^f}{dz} = -\frac{2}{\gamma} \frac{E_m(w_b^m - w_a^m)}{(1 + \nu_m)(b^2 \ln \frac{b}{a} - a^2/2\gamma)}. \tag{20}$$

By differentiating (20) with respect to z and making use of $\sigma_{zz}^m(b, z)$ given in (18), we obtain the second order differential equation

$$\frac{d^2\bar{\sigma}_{zz}^f}{dz^2} = -\frac{2}{\gamma(1 + \nu_m)} \frac{\frac{\sigma - \bar{\sigma}_{zz}^f}{\beta} - \frac{\sigma_{zz}^m(a, z)}{\gamma\beta}}{b^2 \ln \frac{b}{a} - a^2/2\gamma}. \tag{21}$$

As it is assumed that there is perfect bonding at the interface, i.e., $\epsilon_z^f(a) = \epsilon_z^m(a)$, the stress-strain relationship given in (3a)₁ reduces to

$$\sigma_{zz}^m(a, z) = \alpha \bar{\sigma}_{zz}^f, \tag{22}$$

where

$$\alpha = E_m/E_f. \tag{23}$$

Now, by substituting $\sigma_{zz}^m(a, z)$ from (22) and β from (19) into (21) and after rearranging, we obtain

$$\frac{d^2\bar{\sigma}_{zz}^f}{dz^2} = -\frac{2}{a^2\gamma^2(1+\nu_m)} \frac{\gamma\sigma - (\alpha + \gamma)\bar{\sigma}_{zz}^f}{(\frac{b}{a})^4 \ln \frac{b}{a} - (3b^2 - a^2)/4a^2\gamma}, \tag{24}$$

which may be simplified and written as

$$\frac{d^2\bar{\sigma}_{zz}^f}{dz^2} - C_1\bar{\sigma}_{zz}^f + C_1\frac{\gamma}{\alpha + \gamma}\sigma = 0, \tag{25}$$

where

$$C_1 = \frac{2}{a^2\gamma^2(1+\nu_m)} \frac{\alpha + \gamma}{(\frac{b}{a})^4 \ln \frac{b}{a} - (3b^2 - a^2)/4a^2\gamma}. \tag{26}$$

By using the boundary conditions given in (7), the analytical solution for the average axial stress of CNT may be expressed as

$$\bar{\sigma}_{zz}^f = \left[\frac{(R - \alpha S) \exp(pz) - (R - \alpha/S) \exp(-pz)}{q} + \gamma \right] \frac{\sigma}{\alpha + \gamma}. \tag{27}$$

The solution for the interfacial shear stress can be obtained by using (8) and (24) and written as

$$\tau_i = \left[(R - \alpha S) \exp(pz) + (R - \alpha/S) \exp(-pz) \right] \frac{ap\sigma}{2q(\alpha + \gamma)} \tag{28}$$

where

$$p = C_1^{1/2}, \quad q = 2 \sinh(pL), \quad R = \gamma^2(\alpha + \gamma) - \gamma, \quad S = \exp(-pL). \tag{29}$$

3. Analytical results

To examine the accuracy of the derived analytical formulas, results are presented and compared with available results in the literature. Various values of key parameters, namely the aspect ratio ($AR = L/2a$), radius ratio (b/a), and modulus ratio (α) are considered to examine the effect of these parameters on the axial and interfacial stresses developed in the CNT. In addition, critical values of embedded length (L) and modulus ratio (α) are estimated based on the maximum shear stress developed just before debonding occurs at the interface. Available experimental data for various parameters that are used in the computations of the analytical results are given in Table 1.

F	12.566 nN	E_m	20 Gpa
a	2 nm	E_f	560 GPa
b	12 nm	ν_f	0.28
L	50 nm	ν_m	0.35

Table 1. Parameter values.

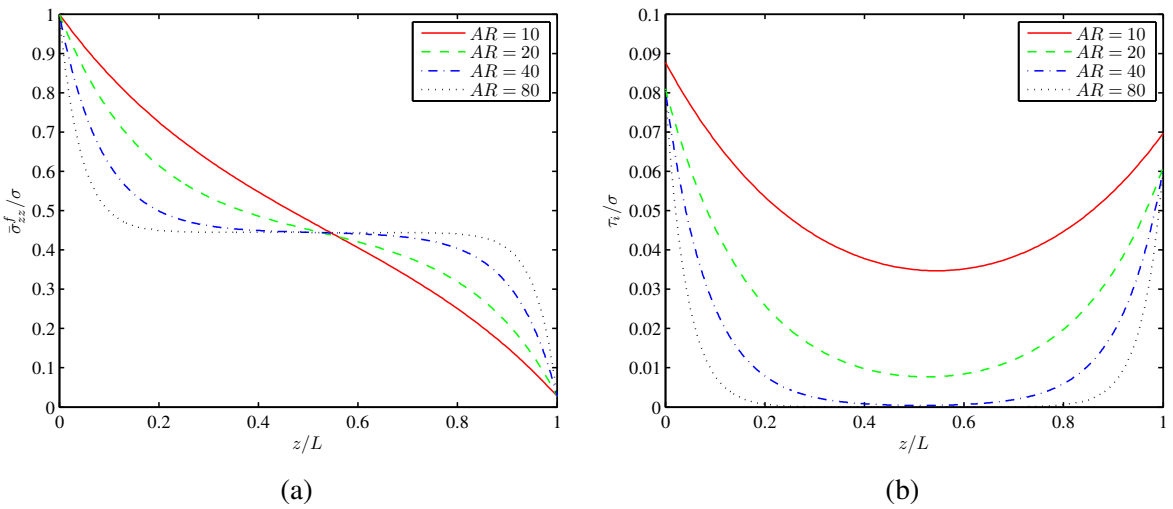


Figure 2. (a) Average axial stress of CNT along the length for different aspect ratios (AR). (b) Interfacial shear stress of CNT along the length for different aspect ratios.

Figure 2 shows the average axial and interfacial shear stress distributions along the length, for different AR. Both the axial and interfacial shear stress distribution trends are quite similar to the recent friction-based pull-out model proposed in [Tan and Kin 2004]. It can be seen from Figure 2a that the axial stress decreases towards the end for all AR. The result also shows that larger stress saturation zone has been found for higher AR. In contrast, the axial stress distributions are linear for smaller AR. This happens because applied stress can be distributed over larger surface area as well as longer length for higher AR. It can be seen from Figure 2b that the shear stress is maximum at $z = 0$. It gradually decreases and reaches the lowest value near the middle of the length. It then gradually increases towards the end. As the uniform stress is applied at $z = 0$, it is to be expected that the interfacial shear stress developed will be maximum at the same location.

Since the tip of the embedded CNT is assumed to be perfectly bonded with the matrix, it is expected that the interfacial shear stress will also show another peak at the tip, i.e., at $z = L$. Figure 2b also shows that the interfacial shear stress tends to be smaller for higher AR. This happens because a higher AR indicates a relatively longer length for a given diameter. Consequently, the shear stress can be distributed over a longer embedded length, thereby resulting in smaller shear stress distribution. It is interesting to note that all the curves in Figure 2b coincide at approximately $z/L = 0.55$. The minimum value of shear stress for all distributions is also noted to occur at this value of z/L .

Figure 3 shows the axial and interfacial shear stress distributions along the length for different radius ratios (b/a). Note that the radius ratio represents different RVE size as well as volume fraction of CNT in the composite. Figure 3a shows that higher axial stress is found for smaller RVE size (smaller b/a). This is to be expected since for a smaller RVE, a bigger proportion of the applied axial stress is to be carried by the CNT. It is also found that the stress distribution is approximately the same for about 10% of the length measured from the open end. The stress distributions deviate significantly from each other in the vicinity of the middle of the embedded length for different (b/a) ratios. Figure 3b shows that

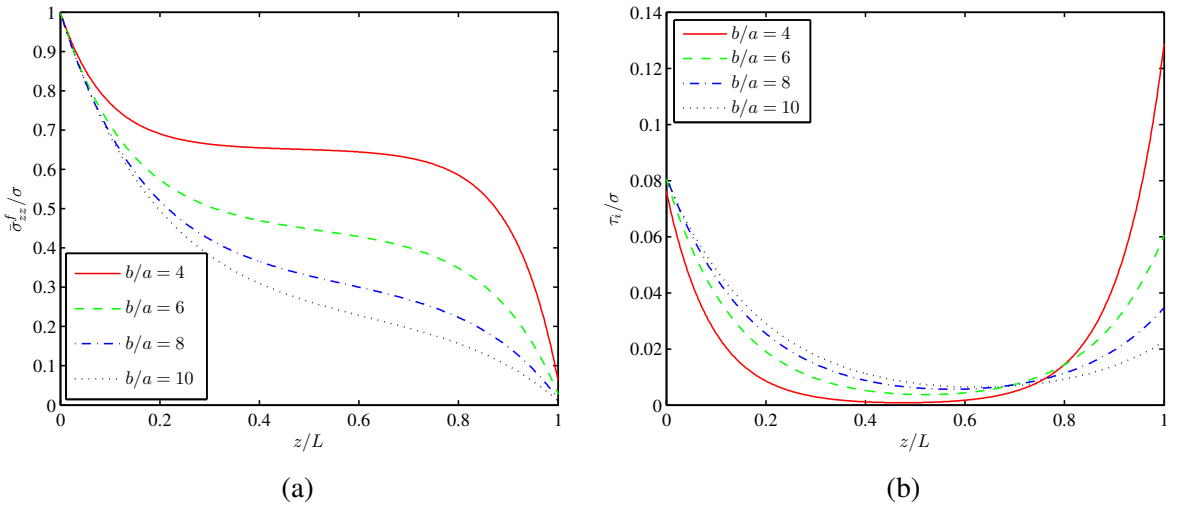


Figure 3. (a) Average axial stress of CNT along the length for different RVE sizes (b/a). (b) Interfacial shear stress of CNT along the length for different RVE sizes.

the interfacial shear stress is close to zero near the middle and rises to large values at the open end and the extreme embedded end. It is also observed that the interfacial shear stress is generally smaller at the extreme embedded end compared to the open end, except when the (b/a) ratio is small. This observation is similar to the results of [Li-Min et al. 1992] for fiber-reinforced composite.

Figure 4 shows the average axial and interfacial shear stress distributions, for different Young's modulus ratios $\alpha = E_m/E_f$ — that is, for different relative matrix strengths. Figure 4a shows that axial stress distribution for any value of α decreases sharply up to 20% of the embedded length from the tip before

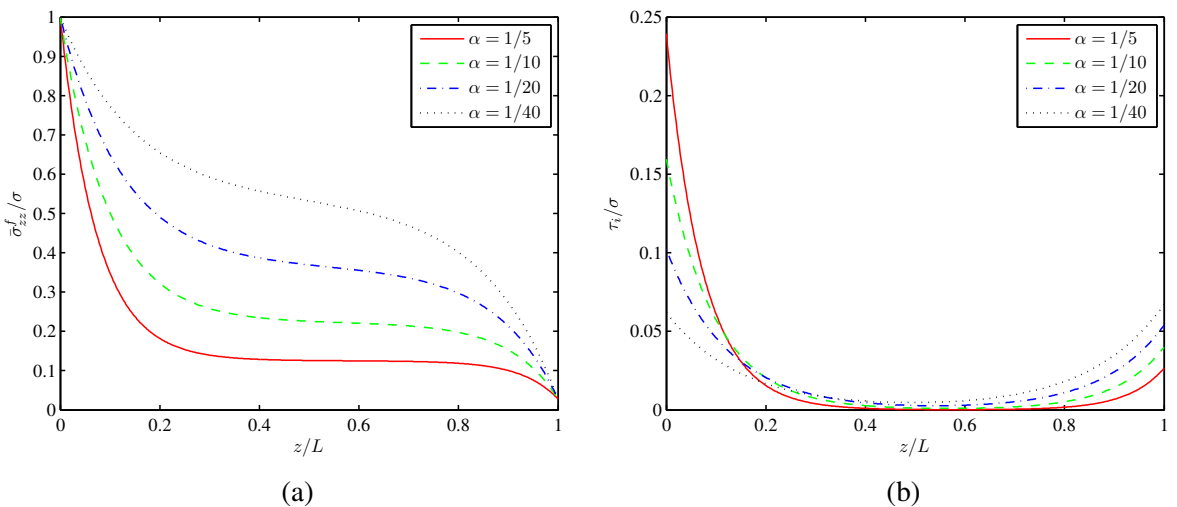


Figure 4. (a) Average axial stress of CNT along the length for different modulus ratios (α). (b) Interfacial shear stress of CNT along the length for different modulus ratios.

reaching a stress constant region and then finally meets a common point at the end. It can be seen from the figure that as larger the value of α is, the axial stress of CNT for different modulus ratios is smaller. For weaker matrix, i.e., smaller modulus ratios, the axial stress distribution is higher as compared to stronger matrix, thereby indicating that the proportion of axial stress carried by CNT decreases as the matrix gets stronger. In contrast, Figure 4b shows that the interfacial shear stress is noted to be virtually zero over most part of the CNT except near the ends with the open end achieving a much larger value than the other end. Interestingly, the interfacial shear stress is noted to be much larger for higher modulus ratios at the open end but the opposite happens at the extreme embedded end.

The current study as well as several previous studies [Ahmed and Ang 2010; Li-Min et al. 1992; Natsuki et al. 2007; Xiao and Liao 2004] show that the maximum interfacial shear stress for the pull-out problem is found at the open end, i.e., at $z = 0$. Thus, it is expected that debonding between the CNT and the matrix will occur at the open end. By rearranging (27), the critical pull-out stress (σ_{cr}) defined as the maximum pull-out force per unit cross-sectional area of CNT at impending debonding can be determined as a function of the allowable interfacial shear stress as follows

$$\sigma_{cr} = \frac{2(\alpha + \gamma)}{ap(2R - \alpha S - \alpha/S)} \tau_{max} \tag{30}$$

The allowable interfacial shear stress is dependent on the nature of the CNT/matrix interface. Manoharan et al. [2009] has measured this value for CNT-reinforced epoxy composite experimentally using a scanning electron microscope to be nearly 200 MPa. Liao and Li [2001] have determined the maximum interfacial shear stress to be about 160 MPa through molecular dynamic simulation on the pull-out problem of a nanotube/polymer system. Knowing the maximum interfacial shear stress (τ_{max}) and other physical and mechanical properties of composite, the critical pull-out stress (σ_{cr}) can be determined using (30).

Based on (30), the critical pull-out stress (σ_{cr}) may be determined for any embedded length of CNT. Figure 5 shows the variation of the critical pull-out stress with the embedded length for the case of an epoxy matrix where the allowable interfacial shear stress is taken to be 200 MPa. It can be seen from the curve shown in Figure 5 that σ_{cr} increases gradually with increasing embedded length up to 20 nm and thereafter stays virtually constant. Hence, it is interesting to note that any increase in the embedded length beyond a critical embedded length is unable to prevent debonding at the open end in view that the shear stress induced has already reached the allowable interfacial stress value. Thus, for the case examined here, the critical embedded length is estimated to be approximately 20 nm.

Figure 6 shows the variation of critical pull-out stress (σ_{cr}) with the CNT/matrix modulus ratio, $\alpha(E_m/E_f)$. It can be seen that the σ_{cr} decreases as the modulus ratio increases which agrees with the friction based model for fiber-reinforced model proposed in [Chiang 2001]. This happens because a higher α represents a stronger matrix. As explained previously, a stronger matrix would result in a larger shear stress at the open end as well as a smaller axial stress induced in the CNT. Consequently, the critical pull-out stress is expected to decrease. The figure also shows that σ_{cr} decreases sharply for smaller values of α and remains nearly constant after $\alpha > 0.3$. Similar to the explanation given with regards to the critical embedded length, there is thus a critical value of the modulus ratio beyond which there is no significant variation in the σ_{cr} . For the case discussed, the critical modulus ratio may be taken to be 0.3.

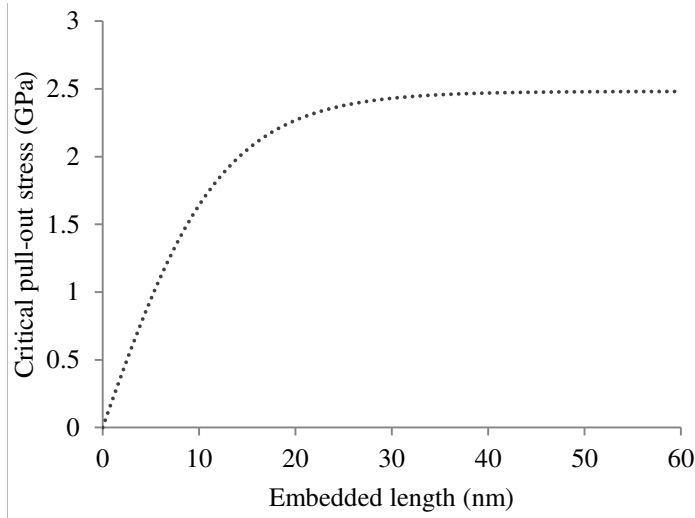


Figure 5. Variation of critical pull-out stress (σ_{cr}) with embedded length (L).

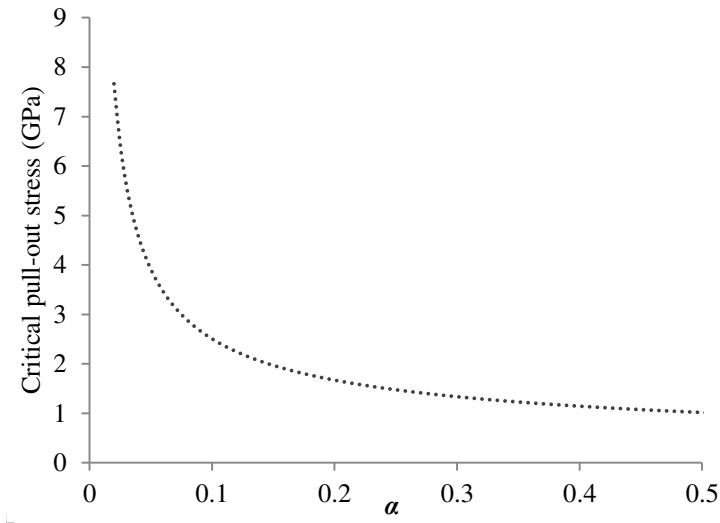


Figure 6. Variation of critical pull-out stress (σ_{cr}) with modulus ratio, α (E_m/E_f).

4. Conclusion

An analytical pull-out model has been proposed to investigate the stress transferring mechanism of CNT in polymer matrix by using classical continuum mechanics. Closed-form solutions have been derived for the axial and interfacial shear stress components. These formulas can be used to investigate the pull-out problem conveniently without resorting to more expensive and complicated experimental study. The present study revealed that the aspect ratio, modulus ratio and radius ratio (RVE size) are the key controlling parameters in CNT-reinforced polymer composites. Critical values of embedded length and modulus ratio for a sample case were also determined, which are the minimum embedded length of CNT

and strongest matrix that can be used effectively with CNT, respectively that correspond to the largest possible pull-out stress for perfectly bonded CNT/polymer interface.

It is to be noted that since we convert the hollow nanotube to be effective solid fiber, the proposed pull-out model is not limited to the CNT-reinforced composite only. The derived solution may therefore be used for other fiber-reinforced composite having similar physical properties, geometric shape and interface.

References

- [Ahmed and Ang 2010] K. S. Ahmed and K. K. Ang, “An improved pull-out model for carbon nanotube reinforced composites”, pp. 41–44 in *Proceedings of the Twenty-third KKCNN Symposium on Civil Engineering* (Taipei, 2010), 2010.
- [Ailin et al. 2010] L. Ailin, K. W. Wang, and C. E. Bakis, “Multiscale damping model for polymeric composites containing carbon nanotube ropes”, *J. Compos. Mater.* **44** (2010), 2301–2323.
- [Ajayan et al. 2000] P. M. Ajayan, L. S. Schadler, C. Giannaris, and A. Rubio, “Single-walled carbon nanotube-polymer composites: strength and weakness”, *Adv. Mater.* **12**:10 (2000), 750–753.
- [Chiang 2001] Y.-C. Chiang, “The influence of Poisson contraction on matrix cracking stress in fiber reinforced ceramics”, *J. Mater. Sci.* **36**:13 (2001), 3239–3246.
- [Cox 1952] H. L. Cox, “The elasticity and strength of paper and other fibrous materials”, *Br. J. Appl. Phys.* **3** (1952), 72–79.
- [Frankland and Harik 2003] S. J. V. Frankland and V. M. Harik, “Analysis of carbon nanotube pull-out from a polymer matrix”, *Surf. Sci.* **525** (2003), L103–L108.
- [Gao and Li 2005] X. Gao and K. Li, “A shear-lag model for carbon nanotube-reinforced polymer composites”, *Int. J. Solids Struct.* **42**:5 (2005), 1649–1667.
- [Haque and Ramasetty 2005] A. Haque and A. Ramasetty, “Theoretical study of stress transfer in carbon nanotube reinforced polymer matrix composites”, *Compos. Struct.* **71**:1 (2005), 68–77.
- [Jiang et al. 2006] L. Jiang, Y. Huang, H. Jiang, G. Ravichandran, H. Gao, K. Hwang, and B. Liu, “A cohesive law for carbon nanotube/polymer interfaces based on the van der Waals force”, *J. Mech. Phys. Solids* **54**:11 (2006), 2436–2452.
- [Jiang et al. 2008] Y. Y. Jiang, W. Zhou, T. Kim, Y. Huang, and J. M. Zuo, “Measurement of radial deformation of single-wall carbon nanotubes induced by intertube van der Waals forces”, *Phys. Rev. B* **77**:15 (2008), Art. ID #153405.
- [Kim and Mai 1998] J.-K. Kim and Y.-W. Mai, *Engineered interfaces in fiber reinforced composites*, Elsevier, Amsterdam, 1998.
- [Kin and Sean 2001] L. Kin and L. Sean, “Interfacial characteristics of a carbon nanotube-polystyrene composite system”, *Appl. Phys. Lett.* **79** (2001), 4225–4227.
- [Kin-tak 2003] L. Kin-tak, “Interfacial bonding characteristics of nanotube/polymer composites”, *Chem. Phys. Lett.* **370** (2003), 399–405.
- [Li-Min et al. 1992] Z. Li-Min, K. Jang-Kyo, and M. Yiu-Wing, “On the single fibre pull-out problem: effect of loading method”, *Compos. Sci. Technol.* **45** (1992), 153–160.
- [Liao and Li 2001] K. Liao and S. Li, “Interfacial characteristics of a carbon nanotube-polystyrene composite system”, *Appl. Phys. Lett.* **79**:25 (2001), 4225–4227.
- [Manoharan et al. 2009] M. P. Manoharan, A. Sharma, A. V. Desai, M. A. Haque, C. E. Bakis, and K. W. Wang, “The interfacial strength of carbon nanofiber epoxy composite using single fiber pull-out experiments”, *Nanotechnology* **20**:29 (2009), Art. ID #295701.
- [Natsuki et al. 2007] T. Natsuki, F. Wang, Q. Q. Ni, and M. Endo, “Interfacial stress transfer of fiber pull-out for carbon nanotubes with a composite coating”, *J. Mater. Sci.* **42**:12 (2007), 4191–4196.
- [Qian 2003] D. Qian, “Load transfer mechanism in carbon nanotube ropes”, *Compos. Sci. Technol.* **63**:11 (2003), 1561–1569.
- [Qian et al. 2000] D. Qian, E. C. Dickey, R. Andrews, and T. Rantell, “Load transfer and deformation mechanisms in carbon nanotube-polystyrene composites”, *Appl. Phys. Lett.* **76**:20 (2000), 2868–2870.

- [Qian et al. 2002] D. Qian, G. J. Wagner, W. K. Liu, M.-F. Yu, and R. S. Ruoff, “Mechanics of carbon nanotubes”, *Appl. Mech. Rev. (ASME)* **55**:6 (2002), 495–533.
- [Salehikhojin and Jalili 2008] A. Salehikhojin and N. Jalili, “A comprehensive model for load transfer in nanotube reinforced piezoelectric polymeric composites subjected to electro-thermo-mechanical loadings”, *Compos. B Eng.* **39**:6 (2008), 986–998.
- [Seshadri and Saigal 2007] M. Seshadri and S. Saigal, “Crack bridging in polymer nanocomposites”, *J. Eng. Mech. (ASCE)* **133**:8 (2007), 911–918.
- [Tan and Kin 2004] X. Tan and L. Kin, “A nonlinear pullout model for unidirectional carbon nanotube-reinforced composites”, *Compos. B Eng.* **35**:3 (2004), 211–217.
- [Thostenson et al. 2001] E. T. Thostenson, Z. Ren, and T.-W. Chou, “Advances in the science and technology of carbon nanotubes and their composites: a review”, *Compos. Sci. Technol.* **61**:13 (2001), 1899–1912.
- [Tserpes et al. 2008] K. Tserpes, P. Papanikos, G. Labeas, and S. Pantelakis, “Multi-scale modeling of tensile behavior of carbon nanotube-reinforced composites”, *Theor. Appl. Fract. Mech.* **49**:1 (2008), 51–60.
- [Wagner 2002] H. D. Wagner, “Nanotube-polymer adhesion: a mechanics approach”, *Chem. Phys. Lett.* **361**:1–2 (2002), 57–61.
- [Wang et al. 2008] W. Wang, P. Ciselli, E. Kuznetsov, T. Peijs, and A. H. Barber, “Effective reinforcement in carbon nanotube-polymer composites”, *Phil. Trans. R. Soc. A* **366** (2008), 1613–1626.
- [Xiao and Liao 2004] T. Xiao and K. Liao, “A nonlinear pull-out model for unidirectional carbon nanotube-reinforced composites”, *Compos. B Eng.* **35**:3 (2004), 211–217.
- [Zheng et al. 2008] Q. Zheng, Q. Xue, K. Yan, X. Gao, Q. Li, and L. Hao, “Effect of chemisorption on the interfacial bonding characteristics of carbon nanotube-polymer composites”, *Polymer* **49**:3 (2008), 800–808.

Received 2 Apr 2012. Revised 29 Sep 2012. Accepted 16 Oct 2012.

KHONDAKER SAKIL AHMED: ksahmed@nus.edu.sg

Department of Civil and Environmental Engineering, 1 Engineering Drive 2, National University of Singapore, Singapore 117576

ANG KOK KENG: cveangkk@nus.edu.sg

Department of Civil and Environmental Engineering, 1 Engineering Drive 2, National University of Singapore, Singapore 117576

JOURNAL OF MECHANICS OF MATERIALS AND STRUCTURES

jomms.net

Founded by Charles R. Steele and Marie-Louise Steele

EDITORS

CHARLES R. STEELE Stanford University, USA
DAVIDE BIGONI University of Trento, Italy
IWONA JASIUK University of Illinois at Urbana-Champaign, USA
YASUHIRO SHINDO Tohoku University, Japan

EDITORIAL BOARD

H. D. BUI École Polytechnique, France
J. P. CARTER University of Sydney, Australia
R. M. CHRISTENSEN Stanford University, USA
G. M. L. GLADWELL University of Waterloo, Canada
D. H. HODGES Georgia Institute of Technology, USA
J. HUTCHINSON Harvard University, USA
C. HWU National Cheng Kung University, Taiwan
B. L. KARIHALOO University of Wales, UK
Y. Y. KIM Seoul National University, Republic of Korea
Z. MROZ Academy of Science, Poland
D. PAMPLONA Universidade Católica do Rio de Janeiro, Brazil
M. B. RUBIN Technion, Haifa, Israel
A. N. SHUPIKOV Ukrainian Academy of Sciences, Ukraine
T. TARNAI University Budapest, Hungary
F. Y. M. WAN University of California, Irvine, USA
P. WRIGGERS Universität Hannover, Germany
W. YANG Tsinghua University, China
F. ZIEGLER Technische Universität Wien, Austria

PRODUCTION production@msp.org

SILVIO LEVY Scientific Editor

Cover design: Alex Scorpan

See <http://jomms.net> for submission guidelines.

JoMMS (ISSN 1559-3959) is published in 10 issues a year. The subscription price for 2012 is US\$555/year for the electronic version, and \$735/year (+ \$60 shipping outside the US) for print and electronic. Subscriptions, requests for back issues, and changes of address should be sent to Mathematical Sciences Publishers, Department of Mathematics, University of California, Berkeley, CA 94720–3840.

JoMMS peer-review and production is managed by EditFLOW[®] from Mathematical Sciences Publishers.

PUBLISHED BY
 **mathematical sciences publishers**
<http://msp.org/>

A NON-PROFIT CORPORATION

Typeset in L^AT_EX

Copyright ©2012 by Mathematical Sciences Publishers

- A model for the shear displacement distribution of a flow line in the adiabatic shear band based on gradient-dependent plasticity**
XUE-BIN WANG and BING MA 735
- A pull-out model for perfectly bonded carbon nanotube in polymer composites**
KHONDAKER SAKIL AHMED and ANG KOK KENG 753
- A perfectly matched layer for peridynamics in two dimensions**
RAYMOND A. WILDMAN and GEORGE A. GAZONAS 765
- Displacement field in an elastic solid with mode-III crack and first-order surface effects**
TAMRAN H. LENGYEL and PETER SCHIAVONE 783
- On the choice of functions spaces in the limit analysis for masonry bodies**
MASSIMILIANO LUCCHESI, MIROSLAV ŠILHAVÝ and NICOLA ZANI 795
- Edge stiffness effects on thin-film laminated double glazing system dynamical behavior by the operational modal analysis**
ALI AKROUT, MARIEM MILADI CHAABANE, LOTFI HAMMAMI and MOHAMED HADDAR 837
- Network evolution model of anisotropic stress softening in filled rubber-like materials**
ROOZBEH DARGAZANY, VU NGOC KHIÊM, UWE NAVRATH and MIKHAIL ITSKOV 861